Feasibility of A Gyroscope-free Inertial Navigation System for Tracking Rigid Body Motion

Chin-Woo Tan, Kirill Mostov, Pravin Varaiya

CALIFORNIA PARTNERS FOR ADVANCED TRANSIT AND HIGHWAYS

Feasibility of a Gyroscope-free Inertial Navigation System for Tracking Rigid Body Motion

Chin-Woo Tan

Kirill Mostov

Pravin Varaiya

Department of Electrical Engineering
and Computer Sciences
University of California, Berkeley
Berkeley, CA 94720
{tan, mostov, varaiya}@robotics.eecs.berkeley.edu

Abstract

We study the feasibility of designing an accelerometer-based gyroscope-free inertial navigation system (INS) that uses *only* accelerometers to compute the linear and angular motions of a rigid body. A model for a micro-machined accelerometer is developed and the accelerometer output equation is derived to relate the linear and angular motions of a rigid body with respect to a fixed inertial frame. A sufficient condition is used to determine if a configuration of accelerometers is feasible. If the condition is satisfied, the angular and linear motions can be computed *separately* using two decoupled equations, one differential and one algebraic. A configuration of six accelerometers distributed on a cube-shaped INS is considered. This configuration is feasible and the angular acceleration is a linear combination of the accelerometer outputs. Based on this six-accelerometer configuration, an algorithm is developed to compute both the angular and linear motions.

Feasibility of a Gyroscope-free Inertial Navigation System for Tracking Rigid Body Motion

1. Introduction

Inertial navigation systems have been widely used in many diverse applications. They include: automobiles, general aviation aircrafts, autonomous flying vehicles such as helicopters, yachts, automated agricultural and construction vehicles, and submarine fleet. Recently, robotics and image stabilisation are among some of the emerging areas that use micro-machined navigation systems. Most inertial navigation systems use accelerometers to sense linear accelerations and gyroscopes to sense angular velocity. In this report, we study the feasibility of designing an accelerometer-based gyroscope-free inertial navigation system (INS) that uses *only* accelerometers to compute the linear and angular motions of a rigid body. In theory, a minimum of six accelerometers are required for a complete description of a rigid body motion. The key to a solution of this problem is the choice of *location* and *orientation* of the accelerometers. It will be shown that for some ''nice'' (or feasible) configurations of accelerometers, the angular and linear motions can be computed separately using two decoupled equations.

The relation between accuracy and price characteristics for different modern gyroscopes is shown in Figure 1.1. It shows that low-cost gyroscopes lack the accuracy that is needed for precise navigation applications. Indeed, it has been reported in ([2], [4]) that, due to challenges associated with micro-miniaturisation of gyroscopes, inexpensive batch-processed gyroscopes cannot achieve the required levels of precision in the near future. A precise micro-machined accelerometer, on the other hand, is more affordable. In fact, this type of accelerometer has become one of the most notable applications of poly-silicon surface-micromachining [5]. Due to recent breakthrough developments in micro-machining technology, the costs of micro-machined accelerometers is decreasing while their accuracy characteristics is being improved. Existing forecasts have indicated that this trend will continue ([3], [8]). Also technically, there are far less fundamental physical con-

straints that inhibit the precision of a micro-machined accelerometer than those that inhibit the precision of a micro-machined gyroscope. So there is a potentially promising market for developing accelerometer-based gyroscope-free inertial navigation systems.
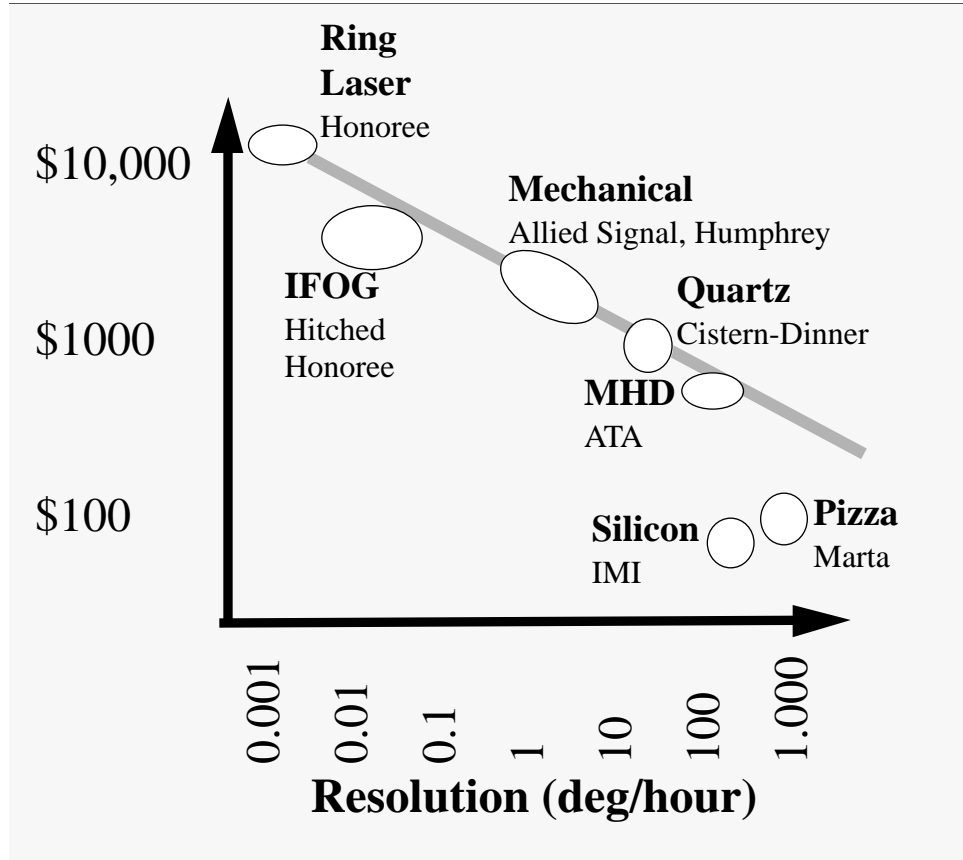

Figure 1.1: Accuracy and price characteristics of gyroscopes

The realisation of a gyroscope-free INS begins with: (1) the development of the main principles of a gyro-free INS design, (2) the development of algorithms derived from the principles for estimating navigation parameters. Semiconductor micro-machined accelerometers are used as basic, sensing devices for an accelerometer-based gyro-free INS. Using measurements from accelerometers strategically distributed on a rigid body (e.g. a vehicle), a gyro-free INS algorithm estimates the body's motion along the six degrees of freedom (linear displacement and rotation of the body with respect to an inertial reference frame). The next section discusses a mathematical model for a semiconductor accelerometer. Rigid body motion equations are derived in Section 3. A sufficient condition is used in Section 4 to determine if a configuration of accelerometers is feasible. A feasible configuration of six accelerometers will be considered in Section 5, and based

on this configuration, a basic gyro-free INS algorithm will be developed. Future work that involves mainly algorithms for correcting INS measurement errors caused by various sources are discussed in Section 6.

2. Modelling of an Accelerometer Sensor

A single axis accelerometer is a device with one input and one output that measures its acceleration along a specific sensing axis. This electro-mechanical device is designed to measure the physical quantity of acceleration of a rigid body to which it is firmly attached, producing an electronic signal proportional to the projection of acceleration along the sensing axis of the accelerometer. The projection of the acceleration vector is a signed variable with its absolute value depending on the orientation and dynamics of the accelerometer. If the velocity of the accelerometer is not changing in the inertial frame of reference associated with the Earth, then the output of an accelerometer remains constant. In addition to measuring changes in velocity, an accelerometer can also measure the projection of gravity onto its sensing axis. Therefore at any given moment the output of an accelerometer measures the projection of the vector sum of the gravity and the projection of acceleration induced by changes in body velocity. The physical structure of a single axis accelerometer and its mathematical model are presented next.

2.1 General Physical Structure

An accelerometer generally consists of a proof mass suspended by compliant beams attached to the rigid body. A simplified model of a single-axis accelerometer consists of a proof mass M and two suspension beams that have an effective spring constant k. There is a damping factor D which affects the movement of the mass. Typically, an accelerometer is modelled by a second-order mass-spring-damper system as shown in Figure 2.1.

The input to the accelerometer is the force that acts on the mass M and causes it to move. Because of the *guides*, the motion of the mass is restricted to a specified sensing direction, which is shown as the x-axis in Figure 2.1. Therefore the device measures the acceleration x_a along the sensing direction x-axis. Customized electronic circuits can

measure any change in x_a, and generate a voltage signal proportional to x_a which is the output of the accelerometer.
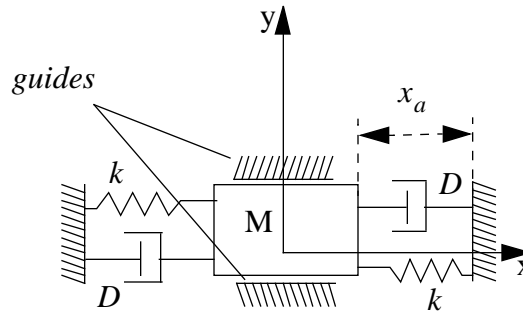

Figure 2.1: General accelerometer structure and its mechanical model.

Without the loss of generality, one can neglect the damping D, since the dynamic response of a typical modern micro-accelerometer exceeds most rigid body dynamics by at least an order of magnitude (i.e. 3000Hz vs. 100Hz). So the dynamics has a *small time constant*. This assumption holds for all vehicles operating at different speeds.

We note that for various emerging applications, the need for high bandwidth (BW) could result in higher noise. However, if the device BW and rigid body dynamics become comparable, we can model the effect of damping by a simple low-pass filter. Taking into account the assumption about damping D, the relationships between the acceleration, force, motion of the mass, and output of the accelerometer can be conceived using the simple mechanical system shown in Figure 2.2.
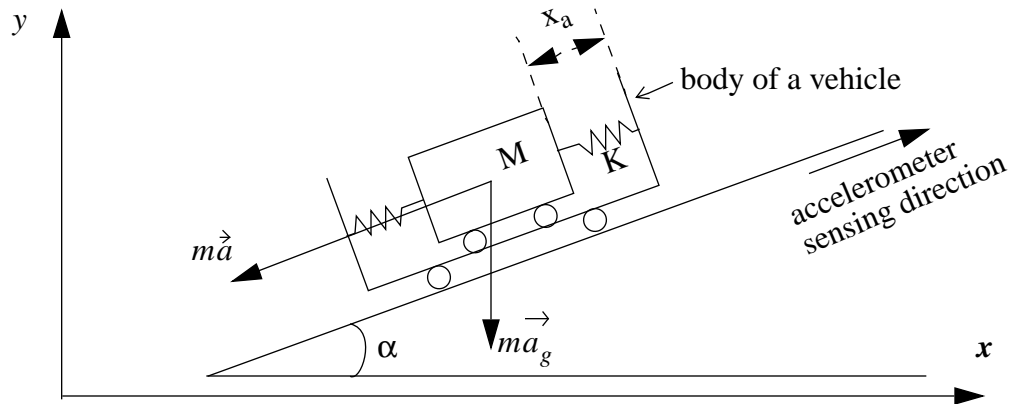

Figure 2.2: Forces exerted on the proof mass

In Figure 2.2 the accelerometer is firmly attached to the body of a vehicle which is moving along a surface inclined at an angle α relative to the x axis. The angle α corresponds to the sensing direction of the accelerometer. The two forces acting on the proof mass are the gravitational force and the force on the vehicle. Newton's second law gives:

$$\vec{F} = m \cdot \vec{a} + m \cdot \vec{ag} = m \cdot (\vec{a} + \vec{a_g}) = m \cdot \vec{a_{eq}}. \tag{2.1}$$

Here the acceleration $\vec{a_{eq}}$ is the vector sum of the accelerations caused by the force on the vehicle and the gravity $\vec{a_g} = 9.8 (m/s^2)$. The accelerometer measures the projection of $\vec{a_{eq}}$ onto its sensing axis given by the inclination angle α.

In order to analyse the measurement mechanism, a model for the spring that suspends the proof mass must be created. If the absolute value of acceleration does not exceed a certain accelerometer threshold (i.e. 50% full scale range for accelerometer ADXLO5), then a linear model of a perfectly resilient spring can be assumed:

$$F = k \cdot x_a \tag{2.2}$$

Here k is the spring constant and x_a is the displacement as shown in Figure 2.2. Equation (2.2) and the projection of (2.1) onto the accelerometer sensing axis can be equated:

$$k \cdot x_a = m \cdot a_{eq}.$$

Here a_{eq} is the projection of $\vec{a_{eq}}$ on the accelerometer sensing axis. Therefore, the basic equation for the accelerometer is:

$$a_{eq} = \ddot{x}_a = \frac{k \cdot x_a}{m}. \tag{2.3}$$

Equation (2.3) is general for all types of accelerometers. For accelerometers that use the micro-machined technology, two approaches for measuring x_a dominate the market: (i) capacitive sensing, (ii) piezoelectric sensing. These approaches convert mechanical information into electrical signals by methods that are particular to the silicon technology.

The case of measuring x_a using the capacitive mechanism is considered next. We will not discuss the less common piezoresistive mechanism.

2.2 Capacitive Accelerometer Model

As shown in Figure 2.3, a capacitive accelerometer monitors the change in capacitance of the parallel plate capacitive structure placed between the proof mass and the substrate. (Note that the substrate is firmly attached to a rigid body.)
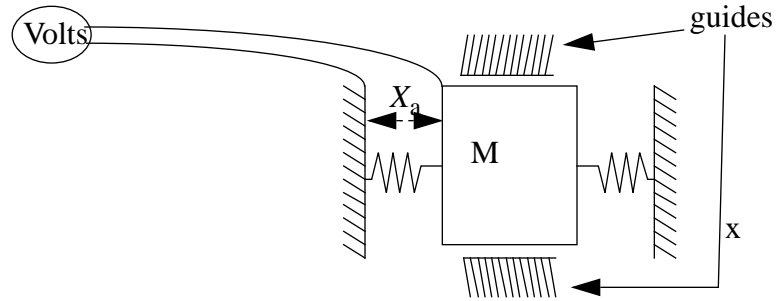
Figure 2.3: Capacitive sensing mechanism

A change in x_a causes a change in the capacitance defined by:

$$C = \varepsilon_o \frac{A}{x_a} \tag{2.4}$$

where ε_o is the permittivity of the air gap, and A is the surface area on either side of the proof mass where the springs are located.

The change in capacitance can be measured by applying an alternating current and measuring its effect on the electrostatic charges across the gap. Equations (2.3) and (2.4) give:

$$a_{eq} = \frac{k \cdot A \cdot \varepsilon_o}{mC} \tag{2.5}$$

which measures the projection of acceleration onto the sensing axis of the device.

2.3 Mathematical Model of an Accelerometer

Figure 2.4 shows a proof body of mass m in its equilibrium state without deflection caused by an input force. Let M be the position of the centre of mass in its equilibrium

state. Let δ denote the x-coordinate of the centre of mass. (Note that the guides limit the body movement to be along the x-axis). Let k be the spring constant.
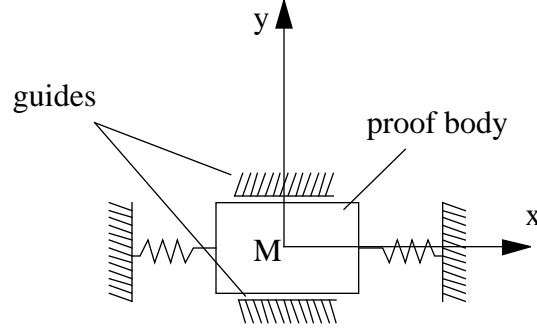

Figure 2.4: Simplified model of an electro-mechanical accelerometer system

Let r_I be the radius-vector of the centre of mass M with respect to a fixed inertial frame, i.e. $r_I \equiv \overrightarrow{O_I M}$, where O_I is the centre of the inertial frame. Let the **unit** vector θ_I be the direction of movement of the accelerometer. This is the sensing direction and is shown as the x-axis in Figure 2.4. When the body rotates θ_I changes in direction with respect to the inertial frame. The position of the centre of mass is given by $r_I + \delta\theta_I$. The proof body is under the influence of the following forces:

1) the resilient force of the springs $f_s = -k\delta\theta_I$,

2) the gravity force $f_g = ma_g$, where a_g is the gravity, and

3) the (total) reaction force from guides f_r. (Note that the reaction force f_r is orthogonal to the x-axis, i.e. $\langle f_r, \theta_I \rangle = 0$).

By equating the forces on the body, the acceleration of the centre of mass is given by:

$$m\left(\ddot{r}_I + \frac{d^2}{dt^2}(\delta\theta_I) \right) = -k\delta\theta_I + ma_g + f_r$$

where t is time. The acceleration in the direction of movement (i.e. sensing direction) is then given by the projection on θ_I, so we have:

$$\langle \ddot{r}_I, \theta_I \rangle + \langle \ddot{\delta}\theta_I + 2\dot{\delta}\dot{\theta}_I + \delta\ddot{\theta}_I, \theta_I \rangle = -\frac{k}{m}\delta\langle\theta_I, \theta_I\rangle + \langle a_g, \theta_I \rangle + \frac{\langle f_r, \theta_I \rangle}{m} \qquad (2.6)$$

Since $\langle\theta_I, \theta_I\rangle = 1$, we have $\langle\dot{\theta}_I, \theta_I\rangle = 0$. Substituting these into (2.6) gives:

$$\langle \ddot{r}_I, \theta_I \rangle + \ddot{\delta} + \delta\langle\ddot{\theta}_I, \theta_I\rangle = -\frac{k}{m}\delta + \langle a_g, \theta_I \rangle$$

This formula can be rewritten as:

$$\langle \ddot{r}_I - a_g + \delta\ddot{\theta}_I, \theta_I \rangle = -\ddot{\delta} - \frac{k}{m}\delta. \qquad (2.7)$$

When a force is applied to the proof mass, the real physical response of the accelerometer is characterised by the proof body displacement $\delta(t)$. (Note that our assumption in damping implies that the time constant of this spring system model is very small. So transients can be ignored.) The accelerometer then produces an output voltage proportional to $\delta(t)$. The right-hand side of equation (2.7) depends only on $\delta(t)$ and contains no motion parameters. All the terms on the left-hand side of (2.7) are motion parameters. Since one observes only the "voltage" output of the accelerometer, one must consider the left-hand side of (2.7) as the "logical" (effective) output of the accelerometer, i.e.

$$A = \langle \ddot{r}_I - a_g + \delta\ddot{\theta}_I, \theta_I \rangle. \qquad (2.8)$$

The logical output of the accelerometer consists of three parts:

$\langle \ddot{r}_I, \theta_I \rangle$ - projection of acceleration of the centre of mass onto the sensing direction,

$\langle a_g, \theta_I \rangle$ - projection of gravitational acceleration onto the sensing direction,

$\langle \delta\ddot{\theta}_I, \theta_I \rangle$ - projection of the product of the displacement and change in the sensing direction over time onto the sensing direction.

Typical values of δ are about 10^{-7} m, so the term $\langle \delta\ddot{\theta}_I, \theta_I \rangle$ is very *small* compared with the other acceleration terms and can be neglected. The accelerometer output (2.8) then becomes:

$$A = \langle \ddot{r}_I - a_g, \theta_I \rangle. \qquad (2.9)$$

In some previous papers ([1], [7]) the logical output is assumed to be only $\langle \ddot{r}_I, \theta_I \rangle$. One must take gravity and change of the sensing direction into account. The inclusion of the effect of gravity is important. Firstly, the gravity vector has constant orientation with respect to the inertial frame; hence it can be used as a reference for calibrating an accelerometer sensing axis. The gravity vector also acts as a reference for calibrating the axes of a body frame relative to the Earth's coordinate frame. Secondly, the presence of gravity leads to significant errors in determining the relative changes in coordinates. A small error in the orientation of a moving frame with respect to the Earth frame can result in a large navigation error. Consider a levelled accelerometer whose sensing direction is off the horizon by an angle $\phi = 0.2$ milli-radian. After $T = 5$ seconds, time integration of this neglected gravity effect will produce a displacement error of the order $a_g \cdot \sin\phi \cdot T^2 \approx 9.8 \cdot (2 \times 10^{-4}) \cdot 5^2$ m. This would exceed errors caused by accelerometer measurement uncertainty. Thus, the effect of gravity cannot be neglected in describing the motion of a rigid body.

3. Rigid Body Motion in R^3

We have discussed in Section 2 that an accelerometer mounted at a point M on a rigid body Σ and pointed at a sensing direction $\theta_I \in R^3$ is a precision instrument designed to measure the acceleration at the point M in the direction θ_I with respect to a fixed inertial frame. In this section, we will describe the motion of a rigid body in R^3 in terms of its linear displacement and rotation relative to an inertial frame. We will present examples of tracking specific types of motion in Section 3.5, and show how accelerometers can be used to determine linear and angular motions in Section 4.

3.1 Rigid Body Motion Equation

In this section we will derive the equations that describe the linear and angular motions of a rigid body with respect to an inertial frame. Without loss of generality, the gravity can be neglected. When an accelerometer is mounted at a point M on the body, the

accelerometer output measures the acceleration at M minus the gravity (see (2.9)). So the gravity term should be included when one considers the output of an accelerometer.
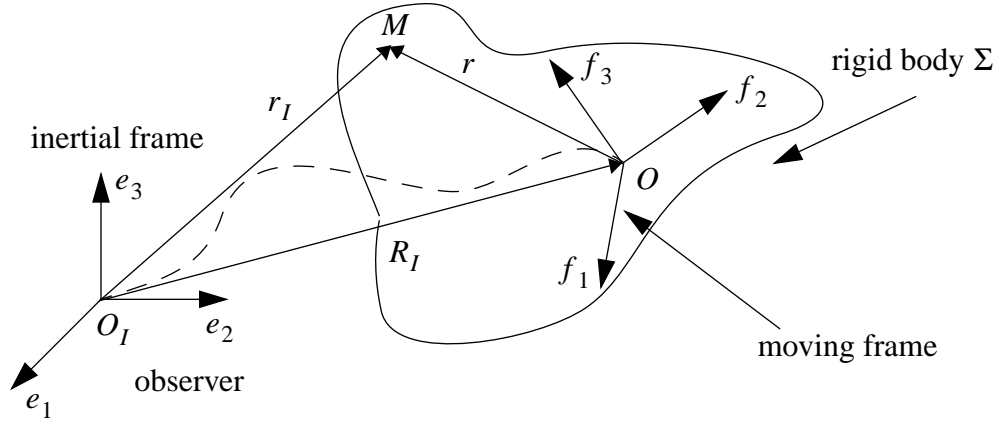

Figure 3.1:   Rigid Body Motion in R^3

Let Σ be a rigid body and M a point of Σ as shown in Figure 3.1. Let O_I be the centre of a ***fixed inertial frame*** with an orthonormal basis $\{e_1, e_2, e_3\}$. (Typically, this is the standard basis in R^3.) We also call O_I the observer. The orthonormal inertial frame is right-handed, that is, the cross products $e_1 \times e_2 = e_3$, $e_2 \times e_3 = e_1$, $e_3 \times e_1 = e_2$ hold. The coordinate system $\{O_I \, ; e_1, e_2, e_3\}$ is called the ***inertial frame***. Motion of the body Σ is described by the translation of the centre O and the rotation of a right-handed orthonormal basis $\{f_1, f_2, f_3\}$ with respect to the inertial frame. The coordinate system $\{O; f_1, f_2, f_3\}$ is called the ***moving frame*** associated with the body.

Rigid body motion consists of *translation* and *rotation*. The translation is given by the vector coordinate $R_I \equiv \overrightarrow{O_I O}$ of the center O of the moving frame relative to the inertial frame. The rotation of the rigid body Σ is described by the rotation of the moving frame with respect to the fixed inertial frame, and is described by a matrix F.

The matrix F descibes the relative orientation of the moving basis $\{f_1, f_2, f_3\}$ with respect to the fixed inertial basis $\{e_1, e_2, e_3\}$. That is, $f_k = F e_k$, $k = 1, 2, 3$. Since the

bases $\{e_1, e_2, e_3\}$ and $\{f_1, f_2, f_3\}$ are orthonormal, F is orthogonal with $F^\mathrm{T}F = I$ (identity matrix). It then follows that $det(F) = \pm 1$. Since the moving frame is right-handed, one must have $det(F) = f_1^T(f_2 \times f_3) = 1$. The matrix F is called a ***rotation operator***, or simply, a ***rotation matrix***.

One can now describe the motion of Σ in terms of its translation $R_I(t)$ and its rotation $F(t)$ relative to the inertial frame. Consider the point M of Σ as shown in Figure 3.1. The vector $r_I \equiv \overrightarrow{O_I M}$ is the coordinate of M in the inertial frame. The vector $r \equiv \overrightarrow{OM}$ is the vector from the centre O to M as seen from the observer O_I. Then

$$r_I = R_I + r. \tag{3.1}$$

where all the vectors in (3.1) are measured in the *inertial frame*.

Since Σ is rigid, the magnitude of r (i.e. distance between center O and M) remains the same. However, the direction of r changes when Σ rotates. The coordinates of M in the *moving frame* are given by $u_k = \langle r, f_k \rangle, k = 1, 2, 3$, which are the projections of r onto the basis vectors $\{f_1, f_2, f_3\}$. Again since Σ is rigid, the coordinates of M in the moving frame remain the same, so $u_k(t) \equiv$ constant. Thus $u = \sum_{k=1}^{3} u_k e_k$ is ***independent of time***. (If $\{e_k\}$ is the standard basis, then u is the vector from O to M in the moving frame.) The vector r can be expressed as $\sum_{k=1}^{3} \langle r, f_k \rangle f_k$, so we get

$$r = \sum_{k=1}^{3} \langle r, f_k \rangle f_k = \sum_{k=1}^{3} u_k F e_k = Fu \tag{3.2}$$

Substituting (3.2) into (3.1) gives

$$r_I = R_I + Fu \tag{3.3}$$

Thus the motion of any point of Σ can be described by the translation $R_I(t)$ and rotation $F(t)$ of Σ relative to the *inertial frame*.

The acceleration of the point M (relative to the ***inertial frame***) is given by

$$\ddot{r}_I = \ddot{R}_I + \ddot{F}u \tag{3.4}$$

Since F is orthogonal, we have $F^{\mathrm{T}}F = I$. Time differentiation of this equality gives:

$$F^{\mathrm{T}}\dot{F} + \dot{F}^{\mathrm{T}}F = 0$$

Define $\Omega \equiv F^{\mathrm{T}}\dot{F}$. So Ω is **skew-symmetric** with $\Omega^{\mathrm{T}} = -\Omega$. Also $\Omega \equiv F^{\mathrm{T}}\dot{F}$ and the orthogonality of F imply

$$\dot{F} = F\Omega. \tag{3.5}$$

Differentiating (3.5) with respect to time gives:

$$\ddot{F} = F\dot{\Omega} + \dot{F}\Omega.$$

Using (3.5) we get

$$\ddot{F} = F(\dot{\Omega} + \Omega^2). \tag{3.6}$$

So from (3.4) the acceleration of the point M can also be expressed as:

$$\ddot{r}_I = \ddot{R}_I + F(\dot{\Omega} + \Omega^2)u. \tag{3.7}$$

The output of an accelerometer can be obtained from (3.7), which we will next consider.

3.2 Accelerometer Output

Suppose an accelerometer of the type described in Section 2.3 is attached at a point M of a rigid body Σ. The coordinate and sensing direction of the accelerometer in the **moving frame** are u and θ (a unit vector), respectively. Note that, as explained in Section 3.1, both u and θ are independent of time. The corressponding coordinate and sensing direction in the **inertial frame** are $r = Fu$ and $\theta_I = F\theta$. Equation (2.9) states that the output of the accelerometer is:

$$A = A(r, \theta_I) = \langle \ddot{r}_I - a_g, \theta_I \rangle, \qquad \text{where } r_I = R_I + r \tag{3.8}$$

Using (3.7) for $\ddot{r}_I$ and $\theta_I = F\theta$ in (3.8), the output $A(r, \theta_I)$, expressed as a function of the *time-independent* variables (u, θ), is:

$$A(u, \theta) = \langle (\ddot{R}_I - a_g) + F(\dot{\Omega} + \Omega^2)u, F\theta \rangle$$
$$= \langle F^T(\ddot{R}_I - a_g) + (\dot{\Omega} + \Omega^2)u, \theta \rangle \qquad (3.9)$$
$$= \langle P, \theta \rangle + \langle Gu, \theta \rangle$$

where $P = F^T(\ddot{R}_I - a_g)$ and $G = \dot{\Omega} + \Omega^2$. The term $\langle P, \theta \rangle$ computes the *linear* acceleration (along θ). The other term $\langle Gu, \theta \rangle$ computes the *angular* acceleration which consists of the *tangential* (skew-symmetric $\dot{\Omega}$) and *centripetal* (symmetric Ω^2) accelerations. It will be shown in Section 4 that there are special configurations of accelerometers that allow one to compute $\Omega(t)$, $F(t)$, and the coordinate of the centre of the body $R_I(t)$ in the inertial frame.

The authors in ([1], [7]) have obtained an accelerometer output equation, but that equation does *not* consider the transformation of coordinates between the inertial frame and the moving frame. So their rotation matrix is always the identity matrix.

3.3 Some Properties of Rotation Operators

We recall that at all times t, $F(t)$ satisfy $F(t)F^T(t) = I$ and $det(F(t)) = 1$, and $\Omega(t)$ is skew-symmetric. Let

$$SO(3) = \{F \in R^{3 \times 3}, FF^T = I, det(F) = 1\}.$$

This set is referred to as the *special orthogonal group* or the *rotation group* of R^3. It is straight-forward to check that $SO(3)$ is indeed a group under matrix multiplication. The operator $\Omega = F^T\dot{F}$ is skew-symmetric, so it must have the form

$$\Omega = \begin{bmatrix} 0 & -\omega_3 & \omega_2 \\ \omega_3 & 0 & -\omega_1 \\ -\omega_2 & \omega_1 & 0 \end{bmatrix} \qquad (3.10)$$

The set of 3×3 skew-symmetric matrices is linear subspace of $R^{3 \times 3}$.

Lemma 3.1: *Let $\Omega \in R^{3 \times 3}$. Ω is skew-symmetric if and only if there is a <u>unique</u> $\omega \in R^3$ such that $\Omega a = \omega \times a$ for all $a \in R^3$.*

Proof: Consider a skew-symmetric Ω as given in (3.10). Let $\omega = \begin{bmatrix} \omega_1 & \omega_2 & \omega_3 \end{bmatrix}^T$. For any

$a = \begin{bmatrix} a_1 & a_2 & a_3 \end{bmatrix}^T$, we have

$$\omega \times a = \begin{bmatrix} \omega_2 a_3 - \omega_3 a_2 \\ \omega_3 a_1 - \omega_1 a_3 \\ \omega_1 a_2 - \omega_2 a_1 \end{bmatrix} = \begin{bmatrix} 0 & -\omega_3 & \omega_2 \\ \omega_3 & 0 & -\omega_1 \\ -\omega_2 & \omega_1 & 0 \end{bmatrix} \begin{bmatrix} a_1 \\ a_2 \\ a_3 \end{bmatrix} = \Omega a$$

Conversely, given $\omega \in R^3$, the cross-product $a \to \omega \times a$ is a linear operator, and it has a matrix representation given by the skew-symmetric Ω. ∎

We shall use $\Omega \leftrightarrow \omega$ or $\Omega = S(\omega)$ to denote that ω is the **cross-product equivalence** of the 3×3 skew-symmetric matrix Ω.

Lemma 3.2: *For any $a, b, c \in R^3$, $\langle a, b \times c \rangle = \langle a \times b, c \rangle$. This is the volume of the parallelogram spanned by the vectors a, b and c.*

Proof: Let B be the 3×3 skew-symmetric matrix such that $B \leftrightarrow b$. By Lemma 2.1 and since $B^T = -B$, we get

$$\langle a, b \times c \rangle = a^T(b \times c) = a^T(Bc) = (B^T a)^T c = (-Ba)^T c = \langle a \times b, c \rangle \qquad ∎$$

Consider the case when $\Omega(t) = constant$. Then the solution to the differential equation $\dot{F} = F\Omega$ is given by $F(t) = F(t_0)e^{\Omega t}$, where $F(t_0)$ is the initial condition. As it will become clear later, this solution corresponds to the rotation of a rigid body about a unit vector $\omega \in R^3$, where $\Omega \leftrightarrow k\omega$ and k is a positive scaling constant. The unit vector ω specifies the direction of rotation as given by the right-hand side. To ensure that $F(t_0)e^{\Omega t}$ is a rotation matrix, it suffices to show that $e^{\Omega t}$ is a rotation since $SO(3)$ is a group under matrix multiplication. We first obtain an expression for the exponential $e^{\Omega \theta}$, where Ω is skew-symmetric and $\theta \in R$.

Lemma 3.3: *Let $\Omega \in R^{3 \times 3}$ be skew-symmetric and $\Omega \leftrightarrow \omega$. The following relations*

hold:

$$\Omega^2 = \omega\omega^T - \|\omega\|^2 I \tag{3.11}$$

$$\Omega^3 = -\|\omega\|^2 \Omega \tag{3.12}$$

Higher powers of Ω are given by:

$$\Omega^{2k+1} = (-1)^k \|\omega\|^{2k} \Omega, \ k = 1, 2, 3, \ldots \tag{3.13}$$

$$\Omega^{2k} = (-1)^{k-1} \|\omega\|^{2k-1} \Omega^2, \ k = 2, 3, \ldots \tag{3.14}$$

<u>Proof</u>: The relation $\Omega^2 = \omega\omega^T - \|\omega\|^2 I$ can be verified by direct calculation, where Ω is

given by (3.10) and $\Omega \leftrightarrow \omega$, and $\|\omega\|^2 = \sum_{i=1}^{3} \omega_i^2$. Next, since $\omega \times \omega = 0$, we have

$$\Omega^3 = \Omega \cdot \Omega^2 = \Omega\omega\omega^T - \|\omega\|^2 \Omega = (\omega \times \omega)\omega^T - \|\omega\|^2 \Omega = -\|\omega\|^2 \Omega,$$

Since (3.11) and (3.12) hold, the relationships (3.13) and (3.14) can be shown by induc-

tion. Suppose (3.13) and (3.14) are true for $k = l$. Then for $k = l+1$, we have

$$\begin{aligned}
\Omega^{2(l+1)+1} &= \Omega^{2l+1}\Omega^2 \\
&= (-1)^l \|\omega\|^{2l} \Omega(\omega\omega^T - \|\omega\|^2 I) \\
&= (-1)^{l+1} \|\omega\|^{2(l+1)} \Omega
\end{aligned}$$

since $\Omega\omega = \omega \times \omega = 0$. Also by (2.12) we have

$$\begin{aligned}
\Omega^{2(l+1)} &= \Omega^{2l}\Omega^2 = (-1)^{l-1} \|\omega\|^{2l-1} \Omega^4 \\
&= (-1)^{l-1} \|\omega\|^{2l-1} \Omega(-\|\omega\|^2 \Omega) \\
&= (-1)^l \|\omega\|^{2l+1} \Omega^2
\end{aligned}$$

So the relations (3.13) and (3.14) hold.   ∎

Using the results in Lemma 3.3, one can compute the exponential of a skew-sym-

metric matrix efficiently. This is referred to below as the <u>*Rodrigues' Formula.*</u>

Proposition 3.1: *Let $\Omega \in R^{3 \times 3}$ be skew-symmetric and $\Omega \leftrightarrow \omega$. Let $\theta \in R$. The exponen-*

tial of $\Omega\theta$ is given by

$$e^{\Omega\theta} = I + \frac{\Omega}{\|\omega\|}\sin(\|\omega\|\theta) + \frac{\Omega^2}{\|\omega\|^2}(1 - \cos\|\omega\|\theta) \tag{3.15}$$

Proof: Using (3.13) and (3.14) in Lemma 3.3, we can write $e^{\Omega\theta}$ as:

$$e^{\Omega\theta} = I + \sum_{k=0}^{\infty} \frac{(\Omega\theta)^{2k+1}}{(2k+1)!} + \sum_{k=1}^{\infty} \frac{(\Omega\theta)^{2k}}{(2k)!}$$

$$= I + \sum_{k=0}^{\infty} \frac{(-1)^k \|\omega\|^{2k+1} \theta^{2k+1}}{(2k+1)!} \cdot \frac{\Omega}{\|\omega\|} - \sum_{k=1}^{\infty} \frac{(-1)^k \|\omega\|^{2k} \theta^{2k}}{(2k)!} \cdot \frac{\Omega^2}{\|\omega\|}$$

$$= I + \frac{\Omega}{\|\omega\|} \sin(\|\omega\|\theta) + \frac{\Omega^2}{\|\omega\|}(1 - \cos\|\omega\|\theta)$$

∎

Next we show that the exponential map transforms skew-symmetric matrices into rotation matrices.

Lemma 3.4: *Let $\Omega \in R^{3 \times 3}$ be skew-symmetric and $\theta \in R$. Then $e^{\Omega\theta} \in SO(3)$.*

Proof: Let $F = e^{\Omega\theta}$. Since $\Omega^T = -\Omega$, we have $(e^{\Omega\theta})^{-1} = e^{-\Omega\theta} = e^{\Omega^T\theta} = (e^{\Omega\theta})^T$. So $FF^T = I$ and it follows that $det(F) = \pm 1$. To show that $det(F) = 1$, we first note that the composite map $\beta \to \Omega\beta \to e^{\Omega\beta} \to det(e^{\Omega\beta})$ is continuous and $det(\exp(0)) = 1$. Since $det(F)$ can only take the discrete values ± 1, we conclude that $det(F) = 1$. ∎

So geometrically, a skew-symmetric matrix corresponds to an axis of rotation (via the mapping $\Omega \leftrightarrow \omega$), and the exponential map generates a rotation corresponding to the rotation about the axis ω (relative to the inertial frame) by a specified angle θ. More interestingly, the converse of Lemma 3.4 is also true. That is, every rotation matrix can be expressed as the matrix exponential of some skew-symmetric matrix. A proof of this assertion can be found in [6].

Proposition 3.2 *Let $F \in SO(3)$. There exists $\omega \in R^3$ and $\theta \in R$ such that $F = e^{\Omega\theta}$, where $\Omega = S(\omega)$.*

The components of the vector $\omega\theta \in R^3$ are called the *exponential coordinates* for $F = e^{\Omega\theta}$. Lemma 3.4 and Proposition 3.2 combine to give the following Euler theorem.

Theorem 3.1 (Euler): Any *rotation matrix* $F \in SO(3)$ *is equivalent to a rotation about a fixed axis* $\omega \in R^3$ *through an angle* $\theta \in [0, 2\pi)$.

3.4 Rotation About a Fixed Axis

In this section we will obtain $F(t)$ and $\Omega(t)$ for rotations about fixed axes. First consider the case when a rigid body rotates about the z-axis (i.e. it has only yaw motion) at a constant angular speed γ rad/sec in the anti-clockwise direction. We take the initial moving frame $\{f_1(0), f_2(0), f_3(0)\}$ to be the standard basis $\{e_1, e_2, e_3\}$ in R^3.
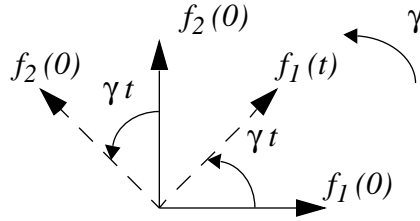

Figure 3.2: Rotation about the z-axis (yaw motion)

As shown in Figure 3.2, after t seconds, the body frame is given by $\{f_1(t), f_2(t), f_3(t)\}$, where

$$f_1(t) = \cos(\gamma t)e_1 + \sin(\gamma t)e_2 = \begin{bmatrix} \cos(\gamma t) \\ \sin(\gamma t) \\ 0 \end{bmatrix}, \quad f_2(t) = \begin{bmatrix} -\sin(\gamma t) \\ \cos(\gamma t) \\ 0 \end{bmatrix}, f_3(t) = \begin{bmatrix} 0 \\ 0 \\ 1 \end{bmatrix}$$

Therefore, the rotation matrix is

$$F_z(t) = [f_1(t), f_2(t), f_3(t)] = \begin{bmatrix} \cos(\gamma t) & -\sin(\gamma t) & 0 \\ \sin(\gamma t) & \cos(\gamma t) & 0 \\ 0 & 0 & 1 \end{bmatrix} \tag{3.16}$$

Next we obtain $\Omega(t)$ which is given by

$$\Omega(t) = F_z(t)^T \dot{F}_z(t) = \gamma \begin{bmatrix} 0 & -1 & 0 \\ 1 & 0 & 0 \\ 0 & 0 & 1 \end{bmatrix} = \gamma \Omega_z \tag{3.17}$$

Recall that for a constant Ω, the solution to $\dot{F} = F\Omega$ is given by $F(t) = F(t_0)e^{\Omega t}$.

So $F_z(t) = e^{\gamma\Omega_z t}$. One can also use the formula (3.15) in Proposition 3.1 to check that $F_z(t)$ is indeed equal to $e^{\gamma\Omega_z t}$. The skew-symmetric matrix Ω_z corresponds to

$$\Omega_z \leftrightarrow \omega_z = \begin{bmatrix} 0 \\ 0 \\ 1 \end{bmatrix}$$

which is the axis of rotation.

Similarly, if a rigid body rotates about the x-axis (i.e. only pitch motion) at a constant speed α in the anti-clockwise direction, then we get

$$F_x(t) = \begin{bmatrix} 1 & 0 & 0 \\ 0 & \cos(\alpha t) & -\sin(\alpha t) \\ 0 & \sin(\alpha t) & \cos(\alpha t) \end{bmatrix},$$

$$\Omega(t) = \alpha \begin{bmatrix} 0 & 0 & 0 \\ 0 & 0 & -1 \\ 0 & 1 & 0 \end{bmatrix} = \alpha\Omega_x \ , \Omega_x \leftrightarrow \omega_x = \begin{bmatrix} 1 \\ 0 \\ 0 \end{bmatrix}, \text{and } F_x(t) = e^{\alpha\Omega_x t}$$

Also, for the case of rotation about the y-axis (i.e. only roll motion) at a constant speed β, we get

$$F_y(t) = \begin{bmatrix} \cos(\beta t) & 0 & \sin(\beta t) \\ 0 & 1 & 0 \\ -\sin(\beta t) & 0 & \cos(\beta t) \end{bmatrix}$$

$$\Omega(t) = \beta \begin{bmatrix} 0 & 0 & 1 \\ 0 & 0 & 0 \\ -1 & 0 & 0 \end{bmatrix} = \beta\Omega_y \ , \Omega_y \leftrightarrow \omega_y = \begin{bmatrix} 0 \\ 1 \\ 0 \end{bmatrix}, \text{and } F_y(t) = e^{\beta\Omega_y t}$$

We note that the rotation matrices about the three basis axes have similar forms. In fact, constant rotations about fixed axes are related by similarity transformations. Consider $\dot{F} = F\Omega$ where Ω is constant; so the body is rotating at a unit speed (1 rad./sec) about an axis ω with $\Omega = S(\omega)$. Let G be the similarity matrix that transform the rotation to that about the z-axis. That is, $\Omega_z = G^T\Omega G$, $GG^T = I$, and $\dot{F}_z = F_z\Omega_z$. Then

$e^{\Omega t} = Ge^{\Omega_z t}G^T$. Since $F(t) = F(t_0)e^{\Omega t}$ and $F_z(t) = F(t_0)e^{\Omega_z t}$, it is immediate that

$$F(t) = F_z(t)G^T.$$

Next consider a rotation about the z-axis. Let $\theta(t)$ be the angle of rotation. Similar to (3.16), the rotation matrix is given by

$$F(t) = \begin{bmatrix} \cos\theta(t) & -\sin\theta(t) & 0 \\ \sin\theta(t) & \cos\theta(t) & 0 \\ 0 & 0 & 1 \end{bmatrix}$$

It is easy to check that

$$\Omega(t) = F(t)^T\dot{F}(t) = \begin{bmatrix} 0 & -\dot\theta(t) & 0 \\ \dot\theta(t) & 0 & 0 \\ 0 & 0 & 0 \end{bmatrix} = \dot\theta(t)\Omega_z \ , \Omega(t) \leftrightarrow \omega(t) = \begin{bmatrix} 0 \\ 0 \\ \dot\theta(t) \end{bmatrix}$$

So for a rigid body rotating about a *fixed* axis, $\omega(t)$ is indeed the body angular velocity. In general, $\omega(t)$ is the *instantaneous angular velocity* of the rotation described by $F(t)$. If we take $\theta(t) = \gamma t$, we get our earlier result of $\Omega(t) = \gamma\Omega_z$ and $F(t) = e^{\gamma\Omega_z t}$. We summarise this in the following lemma.

Lemma 3.5: *Suppose a rigid body rotates around a <u>fixed</u> axis ω_0 with an angular speed $\dot\theta(t)$ so that $\omega(t) = \dot\theta(t)\omega_0$. The corresponding skew-symmetric matrix representation of $\omega(t)$ is $\Omega(t) = \dot\theta(t)\Omega_0$, where $\Omega_0 \leftrightarrow \omega_0$. Then $F(t) = F(t_0)e^{\theta(t)\Omega_0}$ solves the matrix differential equation $\dot{F} = F\Omega, \ t \geq t_0$.*

<u>Proof</u>: It is straight-forward to check that

$$\dot{F}(t) = F(t_0)e^{\theta(t)\Omega_0}\dot\theta(t)\Omega_0 = F(t)\Omega(t) \qquad\qquad \blacksquare$$

3.5 Rigid Body Motion Examples

<u>**Example 1:**</u> Planar circulation and rotation about the vertical axis

Consider a rigid body Σ with centre O_Σ, and an observer at O_I. Initially O_Σ is at a distance δ from O_I. Let $R_I(t)$ be the vector from O_I to O_Σ at time t.
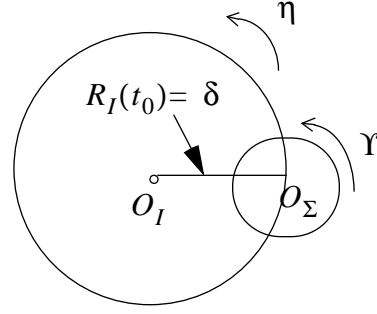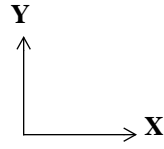
X - Y PLANE

Figure 3.3: Planar circulation and rotation about the vertical axis

The body Σ has two types of motion: (i) Σ circles around the observer O_I on the x-y plane and in the anti-clockwise direction at a constant angular speed η rad/sec. (ii) Σ also rotates about the vertical z-axis at a constant angular speed Υ rad/sec. These two motions are depicted in Figure 3.3. Let $t_0 = 0$ and $R_I(t_0) = \delta e_1$, where the standard basis $\{e_1, e_2, e_3\}$ is the inertial frame at the observer.

Motion (i) is a linear motion, that is, the moving frame (centered at O_Σ) does not rotate with respect to the inertial frame. It is easy to see that

$$R_I(t) = \delta \cos((\eta t)e_1 + \sin(\eta t)e_2)) \tag{3.18}$$

This motion is equivalent to the rotation of the inertial frame about the vertical axis through the observer O_I. So using (3.16)-(3.17) in Section 3.4, we can write $R_I(t)$ as :

$$R_I(t) = R_I(t_0)e^{\eta \Omega_z t} = \delta e^{\eta \Omega_z t} e_1 \quad, \quad \text{where} \quad \Omega_z = \begin{bmatrix} 0 & -1 & 0 \\ 1 & 0 & 0 \\ 0 & 0 & 0 \end{bmatrix}.$$

The linear velocity and linear acceleration of the centre O_Σ are obtained by differentiating (3.18) with respect to time. We get

$$\dot{R}_I(t) = \delta \eta (-\sin(\eta t)e_1 + \cos(\eta t)e_2)$$

$$\ddot{R}_I(t) = -\delta \eta^2 (\cos(\eta t)e_1 + \sin(\eta t)e_2)$$

These formulas can be compacty written as:

$$\dot{R}_I(t) = \delta\eta e^{\eta\Omega_z t} e_2 \quad , \quad \ddot{R}_I(t) = -\delta\eta^2 e^{\eta\Omega_z t} e_1$$

Note that $\ddot{R}_I(t) = -\eta^2 R_I(t)$.

Motion (ii) is a constant angular rotation of the moving frame about the vertical z-axis. So from our discussion in Section 3.4 and (3.16)-(3.17), we have

$$F(t) = e^{\Upsilon\Omega_z t} = \begin{bmatrix} \cos(\Upsilon t) & -\sin(\Upsilon t) & 0 \\ \sin(\Upsilon t) & \cos(\Upsilon t) & 0 \\ 0 & 0 & 1 \end{bmatrix}$$

and

$$\Omega(t) = \Upsilon\Omega_z = \Upsilon \begin{bmatrix} 0 & -1 & 0 \\ 1 & 0 & 0 \\ 0 & 0 & 0 \end{bmatrix} \quad , \quad \Omega_z \leftrightarrow \omega_z = \begin{bmatrix} 0 \\ 0 \\ 1 \end{bmatrix}$$

It is obvious that $\dot{\Omega} = 0$ (since the speed of rotation is constant), so $G = (\dot{\Omega} + \Omega^2) = \Omega^2$.

$$G = \Omega^2 = \Upsilon^2 \begin{bmatrix} -1 & 0 & 0 \\ 0 & -1 & 0 \\ 0 & 0 & 0 \end{bmatrix}$$

The gravity is given by $a_g = -ge_3$. So straight-forward calculations give

$$P = F^T(\ddot{R}_I - a_g) = \begin{bmatrix} \cos(\Upsilon t)\cos(\eta t) + \sin(\Upsilon t)\sin(\eta t) \\ -\sin(\Upsilon t)\cos(\eta t) + \cos(\Upsilon t)\sin(\eta t) \\ g/(-\delta\eta^2) \end{bmatrix} (-\delta\eta^2)$$

When $\eta = \Upsilon$ (i.e. when motions (i) & (ii) are synchronised), we get $P = (-\delta\eta^2)e_1 +$

ge_3 which does not depend on time. ∎

Example 2: Periodic translational and angular accelerations

This example considers a rigid body motion with periodic translational and angular accelerations. The rigid body has two motions: (i) linear acceleration along the x-axis given by a sinusoidal function, and (ii) sinusoidal roll motion about the y-axis.

(i) The linear acceleration along the x-axis is given by:

$$\ddot{R}_I = a_{max} \sin(k_a t) e_1 \qquad (3.19)$$

with initial conditions, $R_I(0) = 0$, $\dot{R}_I(0) = v_o e_1$. Here a_{max}, K_a, v_0 are all positive constants. It is easy to check that

$$\dot{R}_I(t) = \left[\left(v_0 + \frac{a_{max}}{k_a} \right) - \frac{a_{max}}{k_a} \cos(k_a t) \right] e_1$$

and

$$R_I(t) = \left[\left(v_0 + \frac{a_{max}}{k_a} \right) t - \frac{a_{max}}{(k_a)^2} \sin(k_a t) \right] e_1 \qquad .$$

(ii) The sinusoidal roll motion is given by $\omega(t) = \dot{\alpha}(t) e_2$, where $\alpha(t) = \alpha_{max} \sin(k_\alpha t)$ is the angle of rotation and $\dot{\alpha}(t)$ is the angular speed. Then $\Omega(t) = \dot{\alpha}(t) \Omega_y$, where $\Omega_y \leftrightarrow \omega_y = e_2$. By Lemma 3.5 and taking $F(t_0) = I$, we get

$$F(t) = e^{\alpha(t)\Omega_y}$$

By formula (3.15) in Proporition 3.1, we obtain

$$F(t) = e^{\alpha(t)\Omega_y} = \begin{bmatrix} \cos\alpha(t) & 0 & \sin\alpha(t) \\ 0 & 1 & 0 \\ -\sin\alpha(t) & 0 & \cos\alpha(t) \end{bmatrix}$$

Also $\dot{\Omega}(t) = \ddot{\alpha}(t)\Omega_y$. Since $\alpha(t) = \alpha_{max}\sin(k_\alpha t)$, we have $\ddot{\alpha}(t) = -(k_\alpha)^2 \alpha(t)$. So $\dot{\Omega}(t) = -(k_\alpha)^2 \alpha(t)\Omega_y$, and $\dot{\omega}(t) = -(k_\alpha)^2 \alpha(t) e_2$. ∎

4. Feasibility of a Gyro-free INS

A gyroscope-free inertial navigation system (INS) is a system that uses *only* accelerometer measurements to compute the linear displacement and angular rotation of a rigid body. To achieve this, the accelerometers need to be strategically distributed on the rigid body. A set of accelerometers whose outputs are sufficient to calculate the linear and angular motions of a rigid body will be called a *feasible configuration* of accelerometers. In this

section, we will present a sufficient condition for which a configuration is feasible. A feasible configuration for a prototype cube-shaped INS will be considered in Section 5.

Consider N acceleromters mounted at locations $u_1, \ldots, u_N$ of a rigid body Σ with sensing directions $\theta_1, \ldots, \theta_N$, respectively. Recall from Section 3.2 that (u_i, θ_i) are given with respect to the moving frame, and are *time-independent*. From (3.9) the accelerometer output at location u_i is $A_i = A(u_i, \theta_i)$. Recall from Section 3.1 that the motion of *any* point of Σ is described by the translation $R_I(t)$ (coordinate of the centre of the body) and rotation $F(t)$ of Σ relative to the inertial frame. So a gyroscope-free INS needs to be designed in such a way that given the measurements $A_i(t)$ at time t and the initial conditions, one can determine $R_I(t)$ and $F(t)$. This depends on a "good" choice of u_i and θ_i, which we will now define.

<u>Definition 4.1:</u> A configuration $C = \{(u_i, \theta_i); 1 \le i \le N\}$ of N accelerometers mounted on a rigid body is *feasible* if the accelerometer outputs $A_i = A(u_i, \theta_i)$, $1 \le i \le N$, and the initial conditions $\{R_I(t_0), \dot{R}_I(t_0), F(t_0), \dot{F}(t_0)\}$ are sufficient to determine the linear and angular motions, $R_I(t)$ and $F(t)$, for $t \ge t_0$.

Let $J_1 = [u_1 \times \theta_1, \ldots, u_N \times \theta_N]$ and $J_2 = [\theta_1, \ldots, \theta_N]$. (These are $3 \times N$ matrices.) Also let $J = [J_1^T | J_2^T]$, an $N \times 6$ matrix. Using the accelerometer output equation (3.9) and Lemma 3.2, we get

$$A_i = A(u_i, \theta_i) = \langle F^T(\ddot{R}_I - a_g) + (\dot{\Omega} + \Omega^2)u_i, \theta_i \rangle$$

$$= \langle P + \dot{\omega} \times u_i + \Omega^2 u_i, \theta_i \rangle$$

$$= \langle P, \theta_i \rangle + \langle \dot{\omega}, u_i \times \theta_i \rangle + \langle \Omega^2 u_i, \theta_i \rangle$$

$$= \theta_i^T P + (u_i \times \theta_i)^T \dot{\omega} + \theta_i^T \Omega^2 u_i$$

$$= \left[(u_i \times \theta_i)^T \middle| \theta_i^T \right] \begin{bmatrix} \dot{\omega} \\ P \end{bmatrix} + \left[\theta_i^T \Omega^2 u_i \right]$$

So we have

$$A = \begin{bmatrix} A_1 \\ \cdots \\ A_N \end{bmatrix} = J \begin{bmatrix} \dot{\omega} \\ P \end{bmatrix} + \begin{bmatrix} \theta_1^T \Omega^2 u_1 \\ \cdots \\ \theta_N^T \Omega^2 u_N \end{bmatrix} \tag{4.1}$$

If J has a left inverse $Q \in R^{6 \times N}$, then (4.1) becomes

$$\begin{bmatrix} \dot{\omega} \\ P \end{bmatrix} = QA - Q \begin{bmatrix} \theta_1^T \Omega^2 u_1 \\ \cdots \\ \theta_N^T \Omega^2 u_N \end{bmatrix} . \tag{4.2}$$

So $\dot{\omega}$ and $P = F^T(\ddot{R}_I - a_g)$ can be *decoupled* into two systems of equations of the form:

$$\dot{\omega} = f(\omega, A) \tag{4.3}$$

$$P = g(\omega, A) \tag{4.4}$$

Since the matrix differential equation $\dot{F} = F\Omega$ is embedded in (4.2) to relate F and Ω, one can view (4.2) as an **input-output dynamical system** where the *input* is A, the *state equations* are:

$$\dot{\omega} = f(\omega, A); \qquad \dot{F} = F\Omega, \ \Omega \leftrightarrow \omega \quad , \tag{4.5}$$

and the *output equation* is (4.4):

$$P = F^T(\ddot{R}_I - a_g) = g(\omega, A) \quad . \tag{4.6}$$

We note that the state equations are used to compute the angular motion, and the output equation is used to compute the linear motion. So an algorithm for calculating $F(t)$ and $R_I(t)$ is as follows.

Basic Algorithm:

<u>Step 1</u>: Use $F(t_0)$, $\dot{F}(t_0)$ and $\Omega = F^T \dot{F}$, $\Omega \leftrightarrow \omega$, to determine $\omega(t_0)$.

<u>Step 2</u>: Solve (4.3) (numerically) to obtain $\omega(t)$, and thus $\Omega(t)$. (For example, at time t_i, forward Euler approximation of $\dot{\omega}(t)$ gives $\Delta t \cdot \dot{\omega}(t_i) = \omega(t_{i+1}) - \omega(t_i)$.)

<u>Step 3</u>: Solve the matrix differential equation $\dot{F} = F\Omega$ (numerically) to obtain $F(t)$. The solution $F(t_i)$ must be a rotation matrix.

<u>Step 4</u>: Since $P(t)$ is given by the algebraic equation (4.4), the linear displacement $R_I(t)$ can be obtained by using $R_I(t_0)$, $\dot{R}_I(t_0)$ and integrating $\ddot{R}_I(t) = F(t)P(t) + a_g$. That is,

$$R_I(t) = R_I(t_0) + \dot{R}_I(t_0)(t - t_0) + \int_{t_0}^{t}\left[\int_{t_0}^{s}(F(\tau)P(\tau) + a_g)d\tau\right]ds \qquad (4.7)$$

We summarise these computation procedures in the following proposition.

Proposition 4.1 (A sufficient condition for feasibility): If the $N \times 6$ matrix J has a *left inverse*, then the configuration $C = \{(u_i, \theta_i); 1 \le i \le N\}$ is feasible. Also if $N < 6$, then the configuration cannot be feasible.

5. A Six-accelerometer Configuration

For a gyro-free INS, the equations in (4.1) that relate the linear and angular motions are, in general, governed by a set of nonlinear differential equations. These equations are very difficult to solve numerically. There are, however, configurations of accelerometers that would give rise to a set of <u>*decoupled*</u> differential and algebraic equations (4.3)-(4.4) for the angular and linear motions, thus making numerical integration of the decoupled equations feasible. The key to designing a feasible configuration is a good choice of the location and sensing direction of the accelerometers. We shall consider the cube-shaped INS first examined in [1] (despite that their accelerometer output equation is incorrect). The design has one accelerometer at the centre of each face of a cube of length $2L$. The sensing direction of each accelerometer is along the respective cube face diagonal, in such a way that these diagonals form a *regular tetrahedron*. This is shown in Figure 5.1.

Let the origin be the centre of the cube. So the six accelerometers are located at:

$$U = [u_1 ... u_6] = L\begin{bmatrix} 0 & 0 & -1 & 1 & 0 & 0 \\ 0 & -1 & 0 & 0 & 1 & 0 \\ -1 & 0 & 0 & 0 & 0 & 1 \end{bmatrix} \qquad (5.1)$$

The corresponding sensing directions are:

$$J_2 = [\theta_1 ... \theta_6] = \frac{1}{\sqrt{2}} \begin{bmatrix} 1 & 1 & 0 & 0 & -1 & -1 \\ 1 & 0 & 1 & -1 & 0 & 1 \\ 0 & 1 & 1 & 1 & 1 & 0 \end{bmatrix} \qquad (5.2)$$
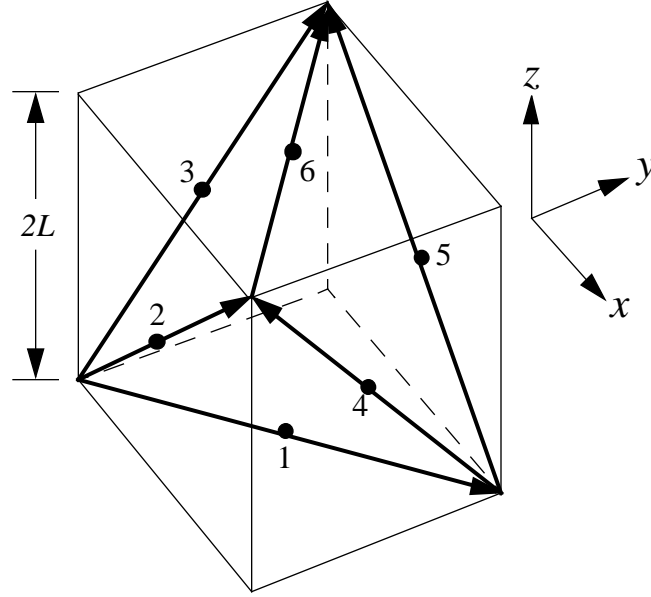

Figure 5.1: A six-accelerometer configuration for a cube-shaped INS

It is easy to check that

$$J_1 = [u_1 \times \theta_1 ... u_6 \times \theta_6] = \frac{L}{\sqrt{2}} \begin{bmatrix} 1 & -1 & 0 & 0 & 1 & -1 \\ -1 & 0 & 1 & -1 & 0 & -1 \\ 0 & 1 & -1 & -1 & 1 & 0 \end{bmatrix} \qquad (5.3)$$

<u>Lemma 5.1</u>: For $i \neq j$, $\frac{1}{L^2} \langle u_i \times \theta_i, u_j \times \theta_j \rangle + \langle \theta_i, \theta_j \rangle = 0$. And each $1 \leq i \leq 6$, we have

$\frac{1}{L^2} \| u_i \times \theta_i \|^2 = 1$ and $\| \theta_i \|^2 = 1$.

<u>Proof</u>: The assertions follow immediately from straight-forward calculations using the J_1

and J_2 matrices. ∎

<u>Proposition 5.1</u>: The inverse of $J = [J_1^T | J_2^T]$ is:

$$Q = J^{-1} = \frac{1}{2}\begin{bmatrix} \frac{1}{L^2}J_1 \\ \\ J_2 \end{bmatrix}.$$ (5.4)

Proof:

$$JQ = \begin{bmatrix} J_1^T & J_2^T \end{bmatrix}\frac{1}{2}\begin{bmatrix} \frac{1}{L^2}J_1 \\ \\ J_2 \end{bmatrix} = \frac{1}{2}\begin{bmatrix} \frac{1}{L^2}J_1^T J_1 + J_2^T J_2 \end{bmatrix}$$

Since $J_1 = [u_1 \times \theta_1 \ldots u_6 \times \theta_6]$ and $J_2 = [\theta_1 \ldots \theta_6]$, the (i, j) entry of JQ is:

$$(JQ)_{ij} = \frac{1}{2}\left[\frac{1}{L^2}(u_i \times \theta_i)^T (u_j \times \theta_j) + \theta_i^T \theta_j\right]$$

$$= \frac{1}{2}\left[\frac{1}{L^2}\langle u_i \times \theta_i, u_j \times \theta_j \rangle + \langle \theta_i, \theta_j \rangle\right]$$

By Lemma 5.1, $(JQ)_{ij}$ is 0 for $i \neq j$, and is 1 for $i = j$. Hence $Q = J^{-1}$. ∎

So by Proposition 4.1, the configuration $C_{cube} = \{(u_i, \theta_i); 1 \leq i \leq 6\}$ is feasible. We next prove the following result which will be useful in obtaining the state equation $\dot{\omega} = f(\omega, A)$ and the output equation $P = g(\omega, A)$.

Lemma 5.2: The second term in the right-hand side of (4.1) is:

$$\begin{bmatrix} \theta_1^T \Omega^2 u_1 \\ \ldots \\ \theta_6^T \Omega^2 u_6 \end{bmatrix} = -LJ_2^T \begin{bmatrix} \omega_2 \omega_3 \\ \omega_1 \omega_3 \\ \omega_1 \omega_2 \end{bmatrix} , \quad \text{where } \Omega \leftrightarrow \omega = \begin{bmatrix} \omega_1 & \omega_2 & \omega_3 \end{bmatrix}^T.$$ (5.5)

Proof: Let $\hat{\omega} = \begin{bmatrix} \omega_2 \omega_3 & \omega_1 \omega_3 & \omega_1 \omega_2 \end{bmatrix}^T$. The u_i and θ_i for configuration C_{cube} are given in (5.1)-(5.2). It is easy to check that:

$$\theta_1^T \Omega^2 u_1 = \frac{L}{\sqrt{2}}(-\omega_1 \omega_3 - \omega_2 \omega_3) = -L\theta_1^T \hat{\omega}$$

$$\theta_2^T \Omega^2 u_2 = \frac{L}{\sqrt{2}}(-\omega_1 \omega_2 - \omega_2 \omega_3) = -L\theta_2^T \hat{\omega}$$

$$\theta_3^T \Omega^2 u_3 = \frac{L}{\sqrt{2}}(-\omega_1\omega_2 - \omega_1\omega_3) = -L\theta_3^T \hat{\omega}$$

$$\theta_4^T \Omega^2 u_4 = \frac{L}{\sqrt{2}}(-\omega_1\omega_2 + \omega_1\omega_3) = -L\theta_4^T \hat{\omega}$$

$$\theta_5^T \Omega^2 u_5 = \frac{L}{\sqrt{2}}(-\omega_1\omega_2 + \omega_2\omega_3) = -L\theta_5^T \hat{\omega}$$

$$\theta_6^T \Omega^2 u_6 = \frac{L}{\sqrt{2}}(-\omega_1\omega_3 + \omega_2\omega_3) = -L\theta_6^T \hat{\omega}$$

Therefore (5.5) holds since $J_2 = \begin{bmatrix} \theta_1 & \dots & \theta_6 \end{bmatrix}$. ∎

<u>Proposition 5.2</u>: The decoupled equations (4.3)-(4.4) for configuration C_{cube} are:

$$\dot{\omega} = \begin{bmatrix} \dot{\omega}_1 \\ \dot{\omega}_2 \\ \dot{\omega}_3 \end{bmatrix} = \frac{1}{2\sqrt{2}L} \begin{bmatrix} A_1 - A_2 + A_5 - A_6 \\ -A_1 + A_3 - A_4 - A_6 \\ A_2 - A_3 - A_4 + A_5 \end{bmatrix} \tag{5.6}$$

$$P = \frac{1}{2\sqrt{2}} \begin{bmatrix} A_1 + A_2 - A_5 - A_6 \\ A_1 + A_3 - A_4 + A_6 \\ A_2 + A_3 + A_4 + A_5 \end{bmatrix} + L \begin{bmatrix} \omega_2\omega_3 \\ \omega_1\omega_3 \\ \omega_1\omega_2 \end{bmatrix} \tag{5.7}$$

<u>Proof</u>: It is easy to check that $J_1 J_2^T = O_3$ and $J_2 J_2^T = 2I_3$, where O_3 is the zero matrix and I_3 is the identity matrix in $R^{3 \times 3}$. So by Proposition 5.1 and Lemma 5.2, we get:

$$Q \begin{bmatrix} \theta_1^T \Omega^2 u_1 \\ \dots \\ \theta_6^T \Omega^2 u_6 \end{bmatrix} = \frac{1}{2} \begin{bmatrix} \frac{1}{L^2} J_1 \\ J_2 \end{bmatrix} \left(-L J_2^T \begin{bmatrix} \omega_2\omega_3 \\ \omega_1\omega_3 \\ \omega_1\omega_2 \end{bmatrix} \right) = -\begin{bmatrix} O_3 \\ L I_3 \end{bmatrix} \begin{bmatrix} \omega_2\omega_3 \\ \omega_1\omega_3 \\ \omega_1\omega_2 \end{bmatrix} \tag{5.8}$$

Substituting (5.8) into (4.2) gives:

$$\begin{bmatrix} \dot{\omega} \\ P \end{bmatrix} = QA - Q \begin{bmatrix} \theta_1^T \Omega^2 u_1 \\ \dots \\ \theta_N^T \Omega^2 u_N \end{bmatrix} = \frac{1}{2} \begin{bmatrix} \frac{1}{L^2} J_1 \\ J_2 \end{bmatrix} \begin{bmatrix} A_1 \\ \dots \\ A_6 \end{bmatrix} + L \begin{bmatrix} O_3 \\ \hat{\omega} \end{bmatrix}$$

where $\hat{\omega} = \begin{bmatrix} \omega_2\omega_3 & \omega_1\omega_3 & \omega_1\omega_2 \end{bmatrix}^T$. Using J_1 in (5.3) and J_2 in (5.2), we obtain (5.6) and (5.7). This completes the proof. ∎

Remarks:

(I) In general, the state equation $\dot{\omega} = f(\omega, A)$ ((4.3)) does not have a closed form solution. To obtain a numerical solution for $\omega(t)$, one needs to approximate $\dot{\omega}$. For the configuration C_{cube}, (5.6) implies that $\dot{\omega}$ is a *linear combination* of the six accelerometer readings. So $\omega(t)$ has a *closed form solution*. This makes numerical integration easier. (Take $\dot{\omega}(t) = A(t)$, so that $\omega(t) = \omega(t_0) + \int_{t_0}^{t} A(\tau)d\tau$. *Forward Euler approximation* of the integral gives $\omega(t_i) = \omega(t_0) + \Delta t \cdot \sum_{j=0}^{i-1} A(t_j)$, where $\Delta t = t_j - t_{j-1}$. This is equivalent to forward Euler approximation of $\dot{\omega}(t)$: $\Delta t \cdot \dot{\omega}(t_i) = \omega(t_{i+1}) - \omega(t_i)$.)

(II) Recall that in the accelerometer output equation (3.9) the term $\langle Gu, \theta \rangle$, where $G = \dot{\Omega} + \Omega^2$, computes the angular acceleration. It consists of the *tangential* (skew-symmetric $\dot{\Omega}$) and *centripetal* (symmetric Ω^2) accelerations. Let us consider the angular acceleration along the x-axis (i.e. $\dot{\omega}_1$). The accelerometers at u_3 and u_4 do not sense motion along the x-axis, so $\dot{\omega}_1$ does *not* depend on these measurements. The *asymmetry* of the sensing directions at $\{u_1, u_6\}$ and $\{u_2, u_5\}$ cancels the symmetric part of the angular motion along the x-axis. That is, the centripetal acceleration $\langle \Omega^2 u_1, \theta_1 \rangle$ measured at u_1 (respectively, $\langle \Omega^2 u_2, \theta_2 \rangle$ measured at u_2) cancels that measured at u_6 (respectively, that measured at u_5). This explains why $\dot{\omega}_1$, the asymmetric part of the angular motion, is a linear combination of the outputs A_1, A_2, A_5 and A_6 .

In conclusion, the basic idea is to first solve the state equations in (4.5) to obtain the angular motion $\omega(t)$, $F(t)$. The output equation (4.6) is then used to obtain the linear motion. These steps are summarised in the Basic Algorithm in Section 4. For the configu-

ration C_{cube}, $\dot{\omega} = f(\omega, A) = f(A)$ is a linear function of A and $P = g(\omega, A)$. They are given in (5.6)-(5.7).

6. Conclusions and Future Work

In this report, a model of a surface micro-machined silicon accelerometer has been derived with the assumptions that are reasonable for applications in road vehicle navigation. This model uses the output voltage of a micro-machined accelerometer device to determine the acceleration of a rigid body along a sensing direction. Rigid body motion equations and the *correct* accelerometer output equation have also been derived. We have also discussed relevant properties of the rotation matrix, and presented two rigid body motion examples. The concept of a feasible configuration of accelerometers is introduced in Section 4. It is shown that for a feasible configuration, the linear and angular motions can be computed separately using two decoupled equations. In principle, there are many feasible configurations. However, for most of them, it is difficult to determine $\omega(t)$ and $\dot{R}_I(t)$ accurately as a result of dependences on values calculated at previous time steps. In Section 5 a set of six accelerometers distributed on the centres of the six faces of a cube is investigated. This configuration is feasible. Moreover, the angular acceleration $\dot{\omega}(t)$ is a linear combination of the accelerometer measurements, thus giving $\omega(t)$ a *closed form solution* and making numerical integration of (4.3) much easier.

To obtain precise estimates of the motion parameters, one must consider the various sources that contribute to the computation errors accumulated in calculating $\omega(t)$ and $F(t)$ (the states in (4.5)), and $R_I(t)$ (the output in (4.6)). These INS error sources are: (i) bias, scale factor errors, (ii) temperature dependent drift, (iii) cross-axis sensitivity errors (between a pair of accelerometers), (iv) location, orientation errors, (v) random device noise, (vi) attitude (reference frame) errors, (vii) numerical integration errors. Errors (i) and (ii) suggest that the measured accelerometer output is indeed a nonlinear function of the true acceleration. This needs to be carefully modelled to reflect the characteristics of the device being used. Errors in (iv) are accelerometer alignment errors. A calibration method needs to be developed to determine these errors, and additional equations need to

be derived to compensate these errors when calculating the motion parameters. Errors in (iii) and (v) will need to be estimated and modelled using experimental data. An algorithm needs to be developed to estimate the error (vi). To update the parameters being corrected in the algorithms that estimate the errors in (i), (ii) and (vi), an external reference (e.g. GPS information) will be needed. Finally, the state equation $\dot{F} = F\Omega$ in general does not have a closed form solution and has to be solved numerically. The numerical scheme must ensure that $F(t)$ is a rotation matrix. The resultant errors from numerical approximations must also be accounted for. Algorithms that estimate or correct these errors will be reported in several future reports.

The algorithms need to be experimentally tested to verify their correctness and accuracy. A brief description of the hardware setup is as follows. The gyroscope-free INS prototype consists of two main parts: (i) six accelerometers distributed on a cube as described in Section 5, (ii) a PC with a special DSP processing board that computes the navigation parameters. Figure 6.1 shows the six-accelerometer cube. The length of each side of the cube is 20 cm. The sensors are accelerometer ADXL05 from Analog Devices. Figure 6.2 shows the complete prototype of the navigation system which consists of the six-sensor cube and the accompanying PC for calculating the navigation parameters, and a rate table for calibration.
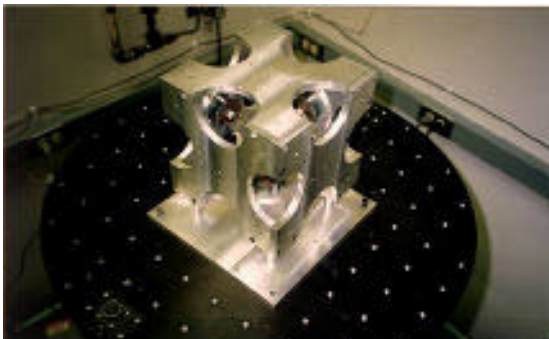

Figure 6.1: A Six-accelerometer multi-sensor system

Figure 6.2: Complete prototype navigation system with a rate table for calibration

The QNX real-time operating system will be used. For this operating system, special attention needs to be given to ensure that the computation processes are synchronised within the QNX framework.

The future work will also include a simulation tool that simulates the algorithms and performs sensitivity analysis. Using a user interface, the simulation tool will allow one to specify the motion of a cube-shaped body and various parameters (e.g. size of the cube, locations and orientations of the accelerometers). It also allows the user to select different levels of accelerometer errors and the discretisation time-step. Suppose the motion of the cube-shaped INS is specified (e.g. constant angular rotation about the vertical axis). One can then compute the accelerometer output readings that correspond to the specified motion. To simlulate the algorithms, one can specify, for example, the location error and the noise level in the sensor device, and then simulate the resultant motion of the body. The simulation results can be used to verify error bounds and sensitivity analyses on parameter values.

References

[1] J-H. Chen, S.-C. Lee, D. B. Debra, ''Gyroscope free Strapdown Inertial Measurement Unit by Six Linear Accelerometers'', *Journal of Guidance, Control, and Dynamics*, Vol. 17, No. 2, pp. 286-290, March-Arpil 1994.

[2] R.L. Greenspan, ''Inertial Navigation Technology from 1970-1995'', *Journal of the Institute of Navigation*, Vol. 42, No. 1, pp.165-185, Spring 1995.

[3] R.T. Howe, B.E. Boser, and R. Horowitz, ''Integrated Micro-Electro-Mechanical Sensor Development for Inertial Applications'', *IEEE Position, Location and Navigation Symposium*, 1998.

[4] A. Kourepenis, J. Borenstein, J. Connelly, R. Elliott, P. Ward, and M. Weinberg, *Performance of MEMS inertial sensors*, New York, NY, USA: IEEE, 1998.

[5] M. A. Lemkin and B. E. Boser, "A 3-axis Force Balanced Accelerometer Using Single Proof Mass", *Proceedings of Tranducers*, pp. 1185-1188, June 1997.

[6] R. Murray, Z. Li, and S. Sastry, *A Mathematical Introduction to Robotic Manipulation*, Boca Raton, CRC Press, 1994.

[7] A. J. Padgaonkar, K. W. Krieger, and A. I. King, "Measurement of Angular Acceleration of a Rigid Body Using Linear Accelerometers", *Journal of Applied Mechanics*, Vol. 42, pp. 552-556, September 1975.

[8] N. Yazdi, F. Ayazi, and K. Najafi, "Micromachined Inertial Sensors", *Proceedings of IEEE*, Vol. 86, No. 8, August 1998.